Inorg. Chem. **2009**, *48*, 3508−3510

Zinc Glycolate: A Precursor to ZnO

Jaykrushna Das,[†] Ivana R. Evans,[‡] and Deepa Khushalani*[,†]

Materials Chemistry Group, Department of Chemical Sciences, Tata Institute of Fundamental Research, Mumbai 400 005, India, and Department of Chemistry, Durham University, Durham DH1 3LE, U.K.

Received January 14, 2009

A simple and versatile solvent-growth process using ethylene glycol has been demonstrated for the synthesis of novel faceted bipyramidal zinc glycolate. Upon thermal treatment in air, this structure can be converted into a ZnO hexagonal phase with wurtzite structure via solid-state transformation. The morphology, microstructure, and crystallinity of the products before and after thermal treatment have been characterized by scanning electron microscopy, X-ray diffraction, Fourier transform infrared spectroscopy, thermogravimetric analysis, and solid-state ^{13}C NMR measurements. In addition, the room-temperature photoluminescence of the resulting ZnO has also been investigated.

In recent years, semiconductor metal oxides have received considerable attention because of their novel properties and versatile technological applications.[1,2] Among these, ZnO is arguably one of the most promising semiconductors. It possesses a room temperature wide band gap of 3.37 eV and a large excitonic (electron−hole) binding energy of 60 meV. This has led to its use in a wide variety of applications such as in catalysis, as piezoelectric devices, and also as an electron transporter in dye-sensitized solar cells.[3−6] The structure in terms of size and morphology is pivotal for all ensuing applications, and developing new synthetic routes to controlling the architecture of such materials has become an important area of research.[7−9]

Different ZnO structures have been synthesized by a range of physical (e.g., vapor−liquid−solid growth, molecular beam epitaxy, chemical vapor deposition, etc.)[10−12] and chemical methods (e.g., precipitation, solvothermal, etc.)[13−18] However, these methods all have some form of drawback because they require either higher processing temperature, sophisticated equipment, and/or adaptability in controlling the high reactivity of the zinc precursors in aqueous media.

With the aim of demonstrating new routes to the formation of ZnO, presented here is the synthesis of a unique intermediate precursor, zinc glycolate, in the presence of ethylene glycol (EG). This novel precursor has been isolated and characterized in detail. The method is an economic, simple procedure in which, typically, 2.73 g of zinc chloride ($ZnCl_2$) and an equimolar amount of sodium hydroxide (NaOH) are added to 100 mL of EG and the mixture is refluxed for 4 h at 190 °C, under a N_2 atmosphere, with stirring. The product is centrifuged, washed with ethanol, and dried at 60 °C for 2 h. It is subsequently calcined at temperatures ranging from 200 to 1000 °C at a rate of 5 °C/min.

Parts a−f of Figure 1 show the temperature evolution of the powder patterns of the precursor with temperature. A detailed room temperature powder X-ray diffraction (XRD) pattern of the precursor material is provided (see Figure S1 in the Supporting Information). In addition to a majority set of intense and sharp peaks, a smaller number of weaker, broad peaks were observed. These were identified as the hexagonal wurtzite form of ZnO. The main set of reflections were indexed to a tetragonal unit with $a = 11.08964(3)$ Å,

* To whom correspondence should be addressed. E-mail: khushalani@tifr.res.in.
[†] Tata Institute of Fundamental Research.
[‡] Durham University.

(1) Kuchibhatla, S. V. N. T.; Karakoti, A. S.; Bera, D.; Seal, S. *Prog. Mater. Sci.* **2007**, *52*, 699–913.
(2) Wang, Z. L. *Annu. Rev. Phys. Chem.* **2004**, *55*, 159–196.
(3) Yu, J. G.; Yu, X. X. *Environ. Sci. Technol.* **2008**, *42*, 4902–4907.
(4) Rout, C. S.; Raju, A. R.; Govindaraj, A.; Rao, C. N. R. *J. Nanosci. Nanotechnol.* **2007**, *7*, 1923–1929.
(5) Law, M.; Greene, L. E.; Johnson, J. C.; Saykally, R.; Yang, P. D. *Nat. Mater.* **2005**, *4*, 455–459.
(6) Pradhan, B.; Batabyal, S. K.; Pal, A. J. *Sol. Energy Mater. Sol. Cells* **2007**, *91*, 769–773.
(7) Wang, Z. L. *J. Phys.: Condens. Matter* **2004**, *16*, R829−R858.
(8) Zheng, Y. H.; Chen, C. Q.; Zhan, Y. Y.; Lin, X. Y.; Zheng, Q.; Wei, K. M.; Zhu, J. F.; Zhu, Y. J. *Inorg. Chem.* **2007**, *46*, 6675–6682.
(9) Gao, P. X.; Wang, Z. L. *J. Am. Chem. Soc.* **2003**, *125*, 11299–11305.
(10) Banerjee, D.; Lao, J. Y.; Wang, D. Z.; Huang, J. Y.; Steeves, D.; Kimball, B.; Ren, Z. F. *Nanotechnology* **2004**, *15*, 404–409.
(11) Umar, A.; Hahn, Y. B. *Nanotechnology* **2006**, *17*, 2174–2180.
(12) Lao, J. Y.; Wen, J. G.; Ren, Z. F. *Nano Lett.* **2002**, *2*, 1287–1291.
(13) Zhang, H.; Wu, J. B.; Zhai, C. X.; Du, N.; Ma, X. Y.; Yang, D. *Nanotechnology* **2007**, *18*, 455604–455610.
(14) Wu, X. F.; Bai, H.; Li, C.; Lu, G. W.; Shi, G. Q. *Chem. Commun.* **2006**, 1655–1657.
(15) Yang, Z.; Liu, Q. H.; Yang, L. *Mater. Res. Bull.* **2007**, *42*, 221–227.
(16) Inoguchi, M.; Suzuki, K.; Kageyama, K.; Takagi, H.; Sakabe, Y. *J. Am. Ceram. Soc.* **2008**, *91*, 3850–3855.
(17) Vafaee, M.; Ghamsari, S. *Mater. Lett.* **2007**, *61*, 3265–3268.
(18) Hartlieb, K.; Raston, C.; Saunders, M. *Chem. Mater.* **2007**, *19* (23), 5453–5459.
(19) Pawley, G. S. *J. Appl. Crystallogr.* **1981**, *14*, 357–361.

10.1021/ic900067w CCC: $40.75 © 2009 American Chemical Society
Published on Web 03/24/2009

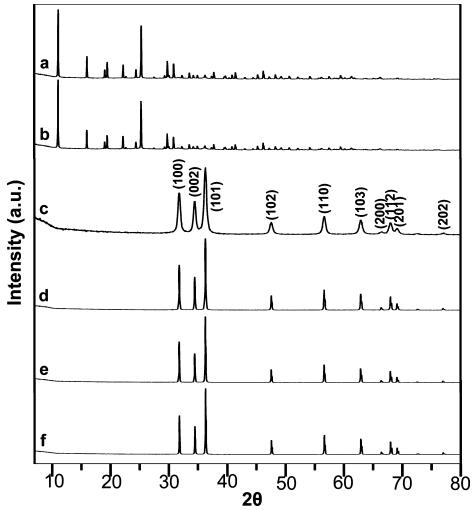

Figure 1. XRD patterns of (a) as-synthesized zinc glycolate and after it has been heated to (b) 200 °C, (c) 400 °C, (d) 600 °C, (e) 800 °C, and (f) 1000 °C.

$c = 11.59010(4)$ Å, and space group $I4_1/a$. The Pawley fit[19] to the pattern using this unit cell and space group is also given in the Supporting Information. Wurtzite was included in the fitting as the second phase, and a final agreement factor $R_{wp} = 3.57\%$ was achieved. A structure solution of zinc glycolate is in progress. It is, however, already clear that this compound is not isostructural with any metal glycolates reported in the Cambridge Structural Database[20] (vanadium glycolate, refcode BARWAT; titanium glycolate, refcode KEPFEQ; titanium/sodium glycolate, refcode YIYLIB).

In Figure 1, the most striking feature is the disappearance of the zinc glycolate peaks above 400 °C (Figure 1c). With further heating, the diffraction peaks of wurtzite ZnO are the only ones present in the pattern; they become more intense and narrow, reflecting an increase in the crystallinity of this phase.

The morphology of the obtained samples before and after calcination was monitored by scanning electron microscopy (SEM), and the representative images are shown in Figure 2. A large number of uniform bipyramidal structures of zinc glycolate were formed (Figure 2a).

This is an intriguing morphology because it has not been observed previously in other zinc complexes. The images confirm that the bipyramidal structure was essentially preserved in the calcination process up to 400 °C (Figure 2c), and an obvious change is seen only after heating to above 400 °C. Clusters, which consisted of a porous, reticulated network, formed once the thermal treatment was carried out to above 600 °C. In situ energy-dispersive X-ray analysis (EDX) confirmed the presence of only zinc as the metal in the final product, and no other contaminants were detected (see Figure S2 in the Supporting Information).

The compositional changes associated with the calcination process were also followed using thermogravimetric analysis (TGA) and Fourier transform infrared (FTIR) spectroscopy (see Figures S3 and S4 in the Supporting Information). The typical TGA and differential thermogravimetry (DTG) curves

(20) Allen, F. H. *Acta Crystallogr. B* **2002**, *58*, 380–388.

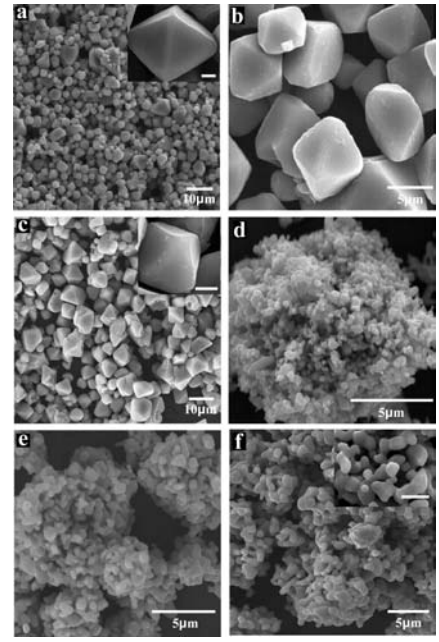

Figure 2. SEM micrographs of (a) zinc glycolate and after it has been heated to (b) 200 °C, (c) 400 °C, (d) 600 °C, (e) 800 °C, and (f) 1000 °C. Inset: enlarged images of parts a, c, and f; the scale bar is 2 μm.

were recorded under a flow of N_2 gas at a heating rate of 5 °C/min. The TGA curve showed a major two-step pattern for weight loss as a function of the temperature. The first weight loss (~2.1%) in the temperature range 25−200 °C was assigned to the loss of physisorbed water and loosely bound EG units, whereas the second one (~29.3% weight loss) in the range of 200−600 °C was attributed to the removal of strong chemically bonded EG (DTG peaks at 347 and 390 °C). It is noteworthy to point out that pure EG gives a sharp, single DTG peak around 213 °C. These two distinct DTG peaks suggest the following: (a) EG is coordinated to zinc such that its decomposition temperature is dramatically increased and there is no unbound EG in the product that is recovered, (b) EG is residing in two distinct chemical environments with respect to zinc, and (c) from the weight loss calculations, a ratio of 1:1 can be determined for Zn:EG.

FTIR studies (see Figure S4 in the Supporting Information) of the as-synthesized zinc glycolate displayed a peak at 1054 cm^{-1}, which was due to the alcoholic C−O stretching mode. Peaks were also observed at 1458 and 1646 cm^{-1}, which were attributed to the O−H bending mode, and a broad band in the region 3000−3500 cm^{-1} was attributed to physically adsorbed water, the EG O−H stretching mode, and any hydrogen bonding between these groups. In addition, a peak at 450 cm^{-1} was assigned to the Zn−O stretching mode. Upon undergoing the calcination treatments, the bands corresponding to O−H and C−H were gradually reduced and eventually disappeared, whereas the Zn−O stretching band was still there but was shifted and broadened. In addition, bands were prevalent between 750 and 1020 cm^{-1}, which corresponded to the bending and twisting vibration of ZnOH. This confirms the fact that the organic moieties were completely removed and only hydroxylated ZnO remained after 400 °C.

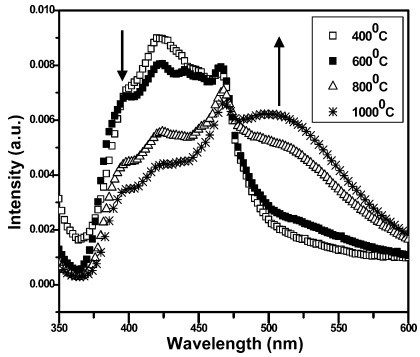

Figure 3. Room temperature PL spectra of ZnO, obtained after annealing at various temperatures as mentioned.

For further insight into the environment of the EG units, solid-state cross-polarization/magic angle spinning ^{13}C NMR was performed (see Figure S5 in the Supporting Information). Two distinctly well-resolved peaks were observed at 64.8 and 65.2 ppm. These were observed at lower field with respect to the standard peak of pure EG at 63.0 ppm, directly suggesting a more deshielded environment of coordinated EG. Also, because two chemical shifts were observed, this correlated with the TGA data that EG was residing in two different chemical environments with respect to zinc.

The room temperature photoluminescence (PL) spectra of ZnO obtained after calcination of zinc glycolate at various temperatures were recorded using the excitation wavelength of 325 nm (Figure 3). When zinc glycolate was annealed to 400 °C, i.e., at the start of the evolution of the ZnO phase (Figure 1c), a weak UV emission at 398 nm was observed that corresponds to the characteristic near-band-edge emission due to free recombination of excitonic centers, which is in accordance with the emission band reported before.[13,21] The visible emission band consists of two well-defined peaks: a strong blue band at ca. 421 nm and a weak blue-green band at ca. 465 nm. Apart from these distinct peaks in the spectrum, a tail at the green emission band is present that is relatively feeble and suppressed. The actual mechanism of the blue and blue-green emissions is not yet well understood, but it is believed that these emissions are possibly due to surface defects in the ZnO powders as described by Greene et al.[22] Furthermore, when the annealing temperature is increased from 600 to 1000 °C, the intensity of the green emission band is dramatically augmented. The result is consistent with the fact that the intensity of the green emission was dramatically enhanced above an annealing temperature of 500 °C for the ZnO film.[23] It can be noted that the origin of the green emission is still unclear, and different hypotheses have been proposed to explain this band. One of the most accepted explanations for the green emission has been associated with oxygen vacancies and vacancy-related defects. Recently, it has also been proposed that the presence of OH species on the surface of oxide is responsible for the green emission.[24] In other words, we presume that both pure and defect-rich ZnO can show green and other visible luminescence depending on the growth temperature and availability of oxygen during the sample preparation.

In summary, we have successively developed a novel solution-grown process to synthesize a unique bipyramidal zinc glycolate precursor using EG as the solvent. From a combination of the characterization techniques used, it is purported that the product consists of EG, which exists in two different chemical environments (bridging and as a bidentate ligand), and the zinc center also has hydroxyl ligands. This precursor provides a route to forming ZnO where both a free exciton UV band and a second deep-level emission band can be tuned depending on the thermal treatment. We believe that this facile nonaqueous route provides a generic method by which a versatile protocol can be developed to prepare morphologically relevant metal oxides.

Acknowledgment. We thank R. S. Thakur for help with the solid-state ^{13}C NMR and Ravi Shukla for assistance with experiments.

Supporting Information Available: Detailed description of materials and methods and figures of the Pawley fit pattern, EDX spectrum, TGA/DTG curves, FTIR spectra, and solid-state ^{13}C NMR spectra. This material is available free of charge via the Internet at http://pubs.acs.org.

IC900067W

(21) Zhong, H. M.; Wang, J. B.; Pan, M.; Wang, S. W.; Li, Z. F.; Xu, W. L.; Chen, X. S.; Lu, W. *Mater. Chem. Phys.* **2006**, *97*, 390–393.
(22) Greene, L. E.; Law, M.; Goldberger, J.; Kim, F.; Johnson, J. C.; Zhang, Y. F.; Saykally, R. J.; Yang, P. D. *Angew. Chem., Int. Ed.* **2003**, *42*, 3031–3034.
(23) Kang, H. S.; Kang, J. S.; Kim, J. W.; Lee, S. Y. *J. Appl. Phys.* **2004**, *95*, 1246–1250.
(24) Reeja-Jayan, B.; De la Rosa, E.; Sepulveda-Guzman, S.; Rodriguez, R. A.; Yacaman, M. J. *J. Phys. Chem. C* **2008**, *112*, 240–246.